Rubisco carboxylase/oxygenase: from the enzyme to the globe: a gas exchange perspective

Humboldt review

Susanne von Caemmerer

Australian Research Council Centre of Excellence for Translational Photosynthesis, Division of Plant Science, Research School of Biology, The Australian National University, Acton, Australian Capital Territory 2601, Australia.

Corresponding author: Susanne von Caemmerer@anu.edu.au

Summary

Rubisco is the primary carboxylase of the photosynthetic process, the most abundant enzyme in the biosphere, and also one of the best-characterized enzymes. Rubisco also functions as an oxygenase, a discovery made 50 years ago by Bill Ogren. Carboxylation of ribulose bisphosphate (RuBP) is the first step of the photosynthetic carbon reduction cycle and leads to the assimilation of CO_2, whereas the oxygenase activity necessitates the recycling of phosphoglycolate through the photorespiratory carbon oxidation cycle with concomitant loss of CO_2. Since the discovery of Rubisco's dual function, the biochemical properties of Rubisco have underpinned the mechanistic mathematical models of photosynthetic CO_2 fixation which link Rubisco kinetic properties to gas exchange of leaves. This has allowed assessments of global CO_2 exchange and predictions of how Rubisco has and will shape the environmental responses of crop and global photosynthesis in future climates. Rubisco's biochemical properties, including its slow catalytic turnover and poor affinity for CO_2, constrain crop growth and therefore improving its activity and regulation and minimising photorespiration are key targets for crop improvement.

1 **Rubisco carboxylase/oxygenase: from the enzyme to the globe: a gas exchange**

2 **perspective**

3

4 Humboldt review

5

6 Susanne von Caemmerer

7 Australian Research Council Centre of Excellence for Translational Photosynthesis, Division

8 of Plant Science, Research School of Biology, The Australian National University, Acton,

9 Australian Capital Territory 2601, Australia.

10 Email address: susanne.caemmerer@anu.edu.au

11 **Abstract**

12 Rubisco is the primary carboxylase of the photosynthetic process, the most abundant

13 enzyme in the biosphere, and also one of the best-characterized enzymes. Rubisco also

14 functions as an oxygenase, a discovery made 50 years ago by Bill Ogren. Carboxylation of

15 ribulose bisphosphate (RuBP) is the first step of the photosynthetic carbon reduction cycle

16 and leads to the assimilation of CO_2, whereas the oxygenase activity necessitates the

17 recycling of phosphoglycolate through the photorespiratory carbon oxidation cycle with

18 concomitant loss of CO_2. Since the discovery of Rubisco's dual function, the biochemical

19 properties of Rubisco have underpinned the mechanistic mathematical models of

20 photosynthetic CO_2 fixation which link Rubisco kinetic properties to gas exchange of leaves.

21 This has allowed assessments of global CO_2 exchange and predictions of how Rubisco has

22 and will shape the environmental responses of crop and global photosynthesis in future

23 climates. Rubisco's biochemical properties, including its slow catalytic turnover and poor

24 affinity for CO_2, constrain crop growth and therefore improving its activity and regulation

25 and minimising photorespiration are key targets for crop improvement.

26

27

28

Introduction

Photosynthetic CO_2 assimilation produces most of the biomass in the biosphere and Rubisco (ribulose 1,5 bisphosphate carboxylase/oxygenase, EC 4.1.1.39) is responsible for the vast majority of global carbon fixation (Raven, 2013). It has been claimed to be the most abundant protein on Earth (Ellis, 1979) and a recent update concludes that the mass of Rubisco on Earth is approximately 0.7 Gt (Bar-On and Milo, 2019). In order to catalyse photosynthetic CO_2 fixation large amounts of Rubisco are needed to compensate for its slow catalytic turnover rate (3-10 s^{-1}), its low affinity for CO_2 in air and low specificity for CO_2 as opposed to O_2 ($S_{c/o}$). Rubisco accounts for at least 20% of leaf nitrogen and its importance in determining the rate of photosynthesis had been recognized early on from correlations between photosynthetic rate and the amount of Rubisco in leaves (Björkman, 1968; Evans and Clarke, 2018; Wareing et al., 1968). Phylogenetic analysis of the Rubisco superfamily supports the existence of at least 3 clades of Rubisco (form I, form II and form III) and it has been suggested that they probably share a common ancestor, most likely that of a methanogenic archaea (Ashida et al., 2008; Iñiguez et al., 2020; Tabita et al., 2008; Whitney et al., 2011). Form I and II can be found among photosynthetic bacteria and Eurkaryotes. Form II Rubiscos are comprised of 2 identical large subunits $(L_2)_n$ and are found in certain photosynthetic bacteria. *Rhodospirillum rubrum*, is a well-studied example (Jordan and Ogren, 1981; Whitney and Andrews, 2001b; Whitney et al., 2011). Form I Rubisco are found in higher plants, algae, cyanobacteria and in autorophic protebacteria. They have a complex quaternary structure composed of eight large (50–55 kD) subunits, which bear the active sites, and eight small (12–18 kD) subunits (Andersson and Backlund, 2008; Portis and Parry, 2007; Roy and Andrews, 2000; Spreitzer and Salvucci, 2002). To function, the Rubisco catalytic site must be carbamylated which occurs through the slow binding of CO_2 to lysine 201 (and this is conserved among all Rubiscos) and this is stabilised through the fast binding of a catalytically essential Mg^{2+} (Andrews and Lorimer, 1987; Lorimer et al., 1976). The interaction of both the carbamylated and non-carbamylated sites with certain sugar phosphates can block and inhibit the active site of the enzyme and requires the action of the ancillary enzyme Rubisco activase (Portis, 2003). A historic perspective of the intriguing discovery of Rubisco activase is provided by Portis and Salvucci (2002). Understandably, Rubisco continues to be studied intensively and is a prime target for genetic engineering to

60   improve photosynthetic efficiency (Parry et al., 2007; Sharwood, 2017) and Portis and Parry

61   (2007) provide a historic perspective on Rubisco research.

62   The aim of this review is to link current research into Rubisco at molecular and biochemical

63   levels with its applications in terrestrial models of photosynthesis and for crop improvement

64   **Rubisco oxygenase activity and the CO_2 compensation point**

65   Photorespiration and the oxygen dependence of CO_2 assimilation rate was investigated in

66   the late sixties and it was shown that the CO_2 compensation point (the CO_2 partial pressure

67   at which no net CO_2 exchange occurs in leaves) was linearly dependent on O_2 concentration.

68   This recognised that the CO_2 compensation point (Γ) represents the balance between

69   photorespiratory CO_2 release and photosynthetic CO_2 uptake (Forrester et al., 1966;

70   Tregunna and Downton, 1967). Looking for a mechanistic explanation for the

71   photorespiratory CO_2 release led to the pivotal discovery that Rubisco was both a

72   carboxylase and oxygenase (Bowes et al., 1971). Ogren (2003) provides a fascinating insight

73   of the discoveries made in his laboratory during that time. It was subsequently shown that

74   the substrates CO_2 and O_2 each behave as competitive inhibitors of the oxygenase and

75   carboxylase reactions respectively (Badger and Andrews, 1974; Bowes and Ogren, 1972;

76   Laing et al., 1974; Peisker, 1974). The inhibition is linearly competitive, which is consistent

77   with both CO_2 and O_2 interacting at a common site.   The rate of carboxylation, V_c, at RuBP

78   saturation has a typical Michaelis-Menten form with respect to the substrate CO_2 and:

79   $$V_c = \frac{C V_{cmax}}{C + K_c(1 + O/K_O)} \qquad (1)$$

80   Where V_{cmax} is the maximal Rubisco carboxylation rate and given by

81   $$V_{cmax} = k_{ccat} E_t \qquad (2)$$

82   and k_{ccat} is the catalytic turnover rate and E_t the total concentration of enzyme sites. K_c and

83   K_O are the Michaelis-Menten constants for the carboxylase and oxygenase. A similar

84   equation for the rate of oxygenation, V_O, can also be written:

85   $$V_O = \frac{O V_{omax}}{O + K_O(1 + C/K_C)} \qquad (3)$$

86   and

87   $$\frac{V_C}{V_O} = \left(\frac{V_{cmax}}{K_c} \frac{K_O}{V_{omax}}\right) \frac{C}{O} = S_{c/o} \frac{C}{O} \qquad (4)$$

88 where $S_{c/o}$ is the Rubisco relative CO_2/O_2 specificity (Laing et al., 1974). The chemical events

89 of carboxylation are now well understood (Tcherkez, 2013), however uncertainty about the

90 chemical mechanism of oxygenation remains (Tcherkez, 2016).

91

92 Laing et al. (1974) were the first to connect leaf gas exchange of soybean leaves with

93 Rubisco kinetic properties and showed that the slope of the O_2 dependence of the CO_2

94 compensation point was proportional to $S_{c/o}$.

95 $$\Gamma_* = \frac{tO}{S_{C/O}} \qquad\qquad\qquad (5)$$

96 The photosynthetic model by Farquhar et al. (1980) used t=0.5. This assumes that for the

97 Rubisco catalysis of one mol of O_2 with one mol of RuBP 0.5 mol of CO_2 are released in the in

98 the photorespiratory carbon oxidation (PCO) cycle. This stoichiometry is embedded in most

99 photosynthetic models, but it has been suggested that the release may be less than 0.5 or

100 more in some instances (Busch, 2020; Hanson and Peterson, 1986; Harley and Sharkey,

101 1991; Zelitch, 1989). It is noteworthy that some photorespiratory mutants have been

102 identified where this stoichiometry is altered (Cousins et al., 2008; Cousins et al., 2011).

103 At the time, Laing et al. (1974) neglected other mitochondrial respiration in the light, R_d. We

104 now recognise the presence of this mitochondrial respiration and the compensation point, Γ

105 is given by a slightly more complex equation

106 $$\Gamma = \frac{\Gamma_* + K_c(1+O/K_O)R_d/V_{cmax}}{1 - R_d/V_{cmax}}, \qquad\qquad (6)$$

107 (Farquhar and von Caemmerer, 1982; von Caemmerer, 2000). Fig. 1a compares Γ and Γ_*

108 and it is evident that there is only a small difference in slope. The full equation helped link

109 ontogenetic and seasonal variation in Γ to the ratio R_d/V_{cmax} (Peisker et al., 1981).

110 Measurements of the compensation point were also used to determine $S_{c/o}$ in conifers

111 where in vitro studies are difficult (Miyazawa et al., 2020). Laisk (1977) developed a

112 technique to estimate Γ_* and R_d from gas exchange measurements and this technique has

113 been used extensively to estimate both parameters (Atkin et al., 2000; Brooks and Farquhar,

114 1985). In these earlier measurements the diffusive conductance from intercellular airspace

115 to the chloroplast (mesophyll conductance) was not considered. von Caemmerer et al.

116 (1994) pointed out that this inclusion was important for accurate estimates of Γ_*, see von

117 Caemmerer (2013) for discussion.

118 The compensation point, Γ, is a robust and easy to measure gas exchange parameter and

119 provides a window into Rubisco's CO_2/O_2 specificity. Interestingly Ogren (2003) reported

120 that attempts to use the compensation point to screen for genetic diversity in oats and a

121 mutagenized soybean population for variation in the balance between photosynthesis and

122 photorespiration were unsuccessful, highlighting how little variation there is in both the

123 parameter t and $S_{c/o}$. In line with this, a recent meta-analysis of Rubisco kinetic parameters

124 measured *in vitro* showed $S_{c/o}$ varied by only 30% amongst Form I Rubiscos and less than

125 10% amongst C_3 plant enzymes (Flamholz et al., 2019).

126 **C_3 photosynthetic models are based on Rubisco kinetic properties**

127 The recognition that Rubisco was an oxygenase as well as a carboxylase led to the

128 development of photosynthetic models based on Rubisco kinetic properties (Farquhar et al.,

129 1980; Hall and Björkman, 1975; Hall, 1979; Laing et al., 1974; Laisk, 1970, 1977; Peisker,

130 1974).

131 Rubisco is localised within the chloroplast stroma and carboxylation of RuBP is the first step

132 of the photosynthetic carbon reduction (PCR) cycle and the carboxylation of 1 mol of RuBP

133 leads to the formation of 2 mol of 3 phosphoglycerate (PGA). The oxygenation of 1 mol of

134 RuBP leads to the formation 1 mol of PGA and 1 mol of phosphoglycolate (PGly) and the

135 recycling of 1 mol of PGly in the photorespiratory carbon oxidation (PCO) cycle leads to the

136 release of 0.5 mol of CO_2 and also includes the release and refixation 0.5 mol of ammonia

137 (Figure 2). This led Farquhar et al. (1980) to write the following equation for CO_2 assimilation

138 rate, *A*:

139 $$A = V_c - 0.5V_0 - R_d, \qquad (7)$$

140 which can be simplified to

141 $$A = (1 - \Gamma_*/C)V_c - R_d \qquad (8)$$

142 with the use of equations 4 and 5. Busch et al., (2018) discuss the stoichiometry of the

143 above equations and possible variations.

144 Substituting equation 1 gives the RuBP saturated or Rubisco limited CO_2 assimilation rate.

145 $$A = \frac{(C - \Gamma_*)}{C + K_c(1 + O/K_O)} V_{cmax} - R_d. \qquad (9)$$

146 In Figure 1b, the Rubisco limited CO_2 assimilation rates are shown at chloroplast CO_2 partial

147 pressures below 250 µbar at 200 and 20 mbar O_2 (ambient and reduced O_2 partial

148 pressures). It is important to note that the reduction in O_2 reduces the photorespiratory

149 CO_2 release but also increases Rubisco carboxylation due to a reduction in the Michaelis

150 Menten constant (equation 9).

151 It was clear early on that the Rubisco limited rate of CO_2 assimilation predicted CO_2

152 assimilation rates much higher than were actually measured at higher CO_2 partial pressures

153 (von Caemmerer and Farquhar, 1981). The formulation of a light limited/electron transport

154 limited CO_2 assimilation rate at higher CO_2 partial pressures or low light was therefore

155 formulated and also based on Rubisco's kinetic properties. *In vitro* kinetics are usually

156 derived with the assumption that the enzyme site concentration is negligible compared to

157 the substrate concentrations. Estimates of Rubisco site concentrations in the chloroplast

158 stroma however range from 2-5 mM and are of the same order of magnitude as RuBP

159 concentrations (Badger et al., 1984; Jensen and Bahr, 1977). Thus in the chloroplast, a large

160 amount of RuBP is bound to Rubisco sites and the standard Michaelis Menten equations do

161 not apply with respect to total chloroplast RuBP concentration. Peisker (1974) was the first

162 to recognise this, but assumed that the Rubisco site concentrations would be greater than

163 RuBP concentrations which we now know is not usually the case (Badger et al., 1984; von

164 Caemmerer and Edmondson, 1986). Farquhar (1979) derived a more general solution and

165 showed that the kinetics with respect to free and bound RuBP are analogous to that which

166 would occur if a tight binding inhibitor was present. The Michaelis Menten equation

167 constant for RuBP is small, approximately 20 µM (Badger and Collatz, 1977; Flamholz et al.,

168 2019; Yeoh et al., 1981). This meant that Rubisco carboxylation or oxygenation could be

169 described as being either RUBP saturated or RuBP limited (Farquhar, 1979; von Caemmerer,

170 2000).

171 When RuBP becomes limiting V_c can be described by an electron transport limited rate that

172 takes into account the NADPH requirement of RuBP regeneration (Figure 2) and the fact

173 that reduction of $NADP^+$ to $NADPH + H^+$ requires the transfer of 2 electrons through the

174 whole chain electron transport thus:

175 $$V_c = \frac{J}{4 + 8\Gamma_*/C} \qquad (10)$$

176 where J is the potential electron transport rate which depends on irradiance. For a more

177 detailed discussion on this and the formulation for an ATP limited rate of electron transport,

178 see von Caemmerer (2000) or Yin et al.(2004). Substituting equation 10 into equation 8

179 gives the electron transport limited rate of CO_2 assimilation:

180 $$A = \frac{(C - \Gamma_*)}{4C + 8\Gamma_*} J - R_d. \qquad (11)$$

181 It is important to note that Γ_* and hence Rubisco specificity, is a player in this equation as it

182 defines the partitioning of NADPH between PCR and PCO cycle. In 21% O, CO_2 assimilation

183 rate continues to increase at higher CO_2 partial pressures as more energy is supporting

184 carboxylation rather than oxygenation as CO_2 partial pressure increases (Figure 1). Both the

185 temperature and O_2 dependence of the quantum yield measured at low light reflect also

186 this competition for energy between the PCR and PCO cycle and this is one of the reasons

187 why $S_{c/o}$ is such an important Rubisco characteristic affecting CO_2 assimilation rate lower in

188 canopies (Ehleringer and Björkman, 1976). This issue was explored in a canopy

189 photosynthesis model to assess how variation in $S_{c/o}$ would play out at the canopy scale (Zhu

190 et al., 2004).

191 The experiments of von Caemmerer and Farquhar (1981) provided at quantitative link

192 between gas exchange measurements of CO_2 assimilation rate and *in vitro* Rubisco kinetic

193 properties and electron transport activity. This led to the now widely used CO_2 response

194 curves of CO_2 assimilation rate (A-Ci curves) as a measure of photosynthetic capacity,

195 particularly in species where enzyme extraction is difficult. To parameterise the model

196 Farquhar et al. (1980) used constants derived from in vitro measurements by Badger and

197 Collatz (1977). von Caemmerer et al. (1994) made use of transgenic tobacco with reduced

198 amounts of Rubisco where CO_2 assimilation rate was RuBP saturated at all CO_2 partial

199 pressures to determine Rubisco kinetic constants in vivo at 25 °C and Bernacchi *et al*. (2002)

200 extended this to derive temperature dependencies which are now used by many (Bernacchi

201 et al., 2013; Sharkey et al., 2007). Together with a temperature dependence of electron

202 transport rate also derived for tobacco there is now a consistent parameterisation of the

203 model (Yamori et al., 2010).

Rubisco's impact on global photosynthesis

Figure 3 highlights the global impact of photosynthesis and Rubisco carboxylation on atmospheric CO_2 concentrations and its isotopic composition. Shown are the monthly averages of atmospheric CO_2 and its carbon isotope composition sampled at Mauna Loa Hawaii (Dlugokencky et al., 2019; White et al., 2018). The figure shows the well-known global rise in atmospheric CO_2 concentration as well as the inter-annual oscillation observed in Mauna Loa Hawaii. Increased photosynthesis in the summer months of the northern hemisphere results in a decrease in atmospheric CO_2. Rubisco's action is apparent in Figure 1b from the concomitant increase in $\delta^{13}C$ which indicates an increase $^{13}CO_2$ in the atmospheric CO_2. Rubisco preferentially fixes $^{12}CO_2$, hence there is a strong isotope signature of Rubisco in atmospheric CO_2. (Farquhar et al., 1989; O'Leary, 1981). It is therefore not surprising that Rubisco is important in the parametrisation of Terrestrial biosphere models (TBM).

A recent review of these models pointed out the impact that the parametrisation of Rubisco kinetic constants has on estimates of terrestrial photosynthesis (Rogers et al., 2017). At present there are few complete data sets for Rubisco kinetic parameters like the tobacco one currently used and although the overall variation of Rubisco kinetic constants is small amongst C_3 species, variation has been observed particularly between cool and warm climate C_3 species and their temperature responses and this deserves further consideration (Flamholz et al., 2019; Galmés et al., 2016; Orr et al., 2016; Sharwood et al., 2016a). New techniques for concurrent measurements of carboxylase and oxygenase using mass spectrometry are being used (Boyd et al., 2018; Boyd et al., 2015; Cousins et al., 2010) but tree species remain underrepresented as it is difficult to extract functional Rubisco for catalytic analysis (Sharwood et al., 2017). Up to now it has been impossible to express the higher plant Rubisco in *E.coli* because of its complex chaperoning requirement for assembly (Bracher et al., 2017; Hayer-Hartl, 2020; Liu et al., 2010). However this hurdle has been overcome for Rubisco from *Arabidopsis thaliana* and partially for *Nicotiana tabacum* and it is likely that this will provide opportunities to study Rubisco kinetic properties from many more species in the near future (Aigner et al., 2017; Wilson et al., 2019).

Terrestrial biosphere or earth system models use photosynthetic capacity, indexed by the maximum Rubisco carboxylation rate (V_{cmax}), to simulate CO_2 assimilation and typically rely

235   on the dependence of V_{cmax} to leaf nitrogen. These have been established for different plant

236   functional types from laborious measurement of leaf nitrogen and A-C_i curves by gas

237   exchange to extract V_{cmax} (Kattge et al., 2009). Maximum electron transport capacity J_{max} is

238   usually scaled with V_{cmax} as the ratio of V_{cmax}/J_{max} is generally conserved when compared at

239   25°C although some variation with leaf N has been observed (Kattge and Knorr, 2007; von

240   Caemmerer and Farquhar, 1981; Walker et al., 2014; Wullschleger, 1993; Yamori et al.,

241   2010; Yamori et al., 2011)

242   When the FvCB model was conceived, the assumption was made that the difference

243   between intercellular CO_2, C_i, and that at Rubisco sites in the chloroplast, C_c, was sufficiently

244   small to be ignored. Subsequently, improved measurements techniques for mesophyll

245   conductance, g_m, the conductance to CO_2 diffusion from intercellular airspace to the site of

246   Rubisco carboxylation in the chloroplast, have shown that it can impose a significant

247   limitation on CO_2 assimilation rate (Flexas et al., 2012; Peguero-Pina et al., 2012; von

248   Caemmerer and Evans, 1991). Furthermore, it varies with temperature and there are

249   significant species differences in the response (von Caemmerer and Evans, 2015). If g_m is

250   not taken into account, V_{cmax} will be underestimated and this affects the V_{cmax}/leaf N

251   relationships. This is currently an issue for the calibration of TBM models that needs to be

252   resolved particularly as the inclusion of g_m in models is essential if carbon isotopic

253   composition of atmospheric CO_2 is to be inferred (Knauer et al., 2020; Suits et al., 2005).

254   Better process knowledge of mesophyll conductance is required and its variation with plant

255   functional types (Gago et al., 2019).

256   Measuring A-C_i curves is time consuming, making it laborious to assess V_{cmax} and Rubisco

257   content in ecosystems or in crops and new measuring techniques are being explored. Rapid

258   measurements of A-Ci curves with new improved portable gas exchange systems have sped

259   up the process, allowing for dynamic measurements during light transitions (Stinziano et al.,

260   2017; Taylor and Long, 2017). An exciting development is the use of hyperspectral

261   reflectance spectroscopy (Furbank et al., 2020; Meacham-Hensold et al., 2019; Serbin et al.,

262   2012; Silva-Perez et al., 2017; Wu, J. et al., 2019). The measurements can be made rapidly

263   and a number of parameters can be extracted such Leaf N, leaf mass per area, V_{cmax} and

264   J_{max}. and dark respiration . However, there is no mechanist basis for the correlation and a

265   large number of hyperspectral reflectance measurements paired with A-C_i curves are

266 needed to build machine learning algorithms. Silva-Perez et al. (2017) were able to screen a

267 large germplasm collection of wheat in different environments. Wu et al. (2019) used the

268 tool in Panamanian tropical rain forest and showed that it was possible to capture seasonal

269 variation in V_{cmax}. It is interesting to note that some studies report that the correlation with

270 hyperspectral reflectance is not driven by the relationship between V_{cmax} and leaf N (Silva-

271 Perez et al., 2017; Wu, J. et al., 2019), This was also shown in a field study that included

272 transgenic tobacco with reduced Rubisco were the correlation between leaf N and V_{cmax}

273 breaks down (Meacham-Hensold et al., 2019). Although Dechant et al. (2017) argue for a

274 link for their diverse tree dataset. Hyperspectral reflectance measurements can also be

275 measured remotely above the leaf canopy (Meacham-Hensold et al., 2020), from drones or

276 planes (Serbin et al., 2015) and possibly in the future from satellites holding promise for

277 capturing seasonal variations in photosynthetic capacity (Alton, 2017).

Rubisco as a target for crop improvement

279 Studies have shown that global crop production needs to double by 2050 to meet the

280 projected demands from a rising population, diet shifts, and increasing biofuels

281 consumption (Ray et al., 2013). Research efforts have focused on improving photosynthesis

282 to improve crop yield (Bailey-Serres et al., 2019; Evans, 2013; Long et al., 2006; Ort et al.,

283 2015; Parry et al., 2013). Improving Rubisco's performance is one of the targets that

284 continues to be considered (Parry et al., 2013; Sharwood, 2017). Efforts include modifying

285 Rubisco kinetic properties, altering its regulation and amount, engineering a high CO_2

286 environment around Rubisco to limit oxygenase activity or manipulating the

287 photorespiratory pathway to reduce CO_2 loss in the photo-respiratory cycle. The last two

288 topics will not be touched on here in detail as there have been excellent recent reviews

289 listed below. A variety of alternative photorespiratory pathways have been engineered into

290 plants initiated by the early work of Kebeish et al.,(2007). The manipulation of the

291 photorespiratory pathway has resulted in biomass increases in tobacco in the field (South et

292 al., 2019). Other opportunities exist and more needs to be learned about the interaction of

293 the photorespiratory pathway with other plant metabolism (Busch, 2020; Sharkey, 2020;

294 South et al., 2018; Timm and Hagemann, 2020). The approaches used to encapsulate

295 Rubisco in high CO_2 environments include the introduction of cyanobacterial or algal

296 biophysical CO_2 concentrating mechanisms (Hennacy and Jonikas, 2020; Long et al., 2018) or

297 the introduction of a complete C_4 photosynthetic pathway (Ermakova et al., 2020).

298 Rubisco engineering itself has been particularly challenging, as plant Rubisco Rubisco is

299 formed from two types of subunits, the small subunits coded for in the nucleus and the

300 large subunit in the plastid genome, however the past decade has seen significant

301 developments from advances in chloroplast engineering and improved understanding of

302 Rubisco biogenesis (Bracher et al., 2017; Sharwood, 2017). Overexpression of Rubisco small

303 subunits in rice has resulted in increased formation of Rubisco holoenzyme which led to

304 yield increases in paddy field experiments when receiving sufficient N fertilisation (Yoon et

305 al., 2020). This is the first field experiment demonstrating the benefits of more Rubisco in a

306 C_3 species.

307 Overexpression of Rubisco large and small subunits with the Rubisco assembly chaperone

308 RAF1 lead to increases in the amount of Rubisco and increased CO_2 assimilation rate as well

309 as mitigate the impact of chilling in the C_4 species, *Z. mays* (Salesse-Smith et al., 2018;

310 Salesse-Smith et al., 2019). The C_4 photosynthetic pathway is a biochemical CO_2

311 concentrating mechanism that involves coordinated functioning of mesophyll (M) and

312 bundle sheath (BS) cells within a leaf. CO_2 is initially assimilated into C_4 acids by

313 phosphoenolpyruvate (PEP) carboxylase in the mesophyll cells. These acids then diffuse to

314 and are decarboxylated in BS cells where CO_2 is concentrated around Rubisco. This allows

315 Rubisco to operate close to its maximal activity and reduces the rate of oxygenation. C_4

316 photosynthesis thus requires much less Rubisco to achieve high photosynthetic rates (Figure

317 4). Modelling of C_4 photosynthesis predicts that an increase in Rubisco activity should

318 increase CO_2 assimilation at ambient and high CO_2 in contrast to C_3 species where Rubisco

319 activity affects CO_2 assimilation rate at lower CO_2 partial pressures (von Caemmerer and

320 Furbank, 2016). A virtual experiment using a crop growth model for wheat (C_3) and

321 Sorghum (C_4) in different environmental scenarios concluded that increasing Rubisco

322 content could be of benefit for both wheat and sorghum depending on the environment

323 during the growing season (Wu, A. et al., 2019).

324 There is great diversity in Rubisco kinetic constants amongst form I Rubisco that can be

325 exploited (Flamholz et al., 2019; Iñiguez et al., 2020). In many instances they have co-

326 evolved with CO_2 concentrating mechanisms, which provide Rubisco with a high CO_2

327 environment (Badger et al., 1998; Iñiguez et al., 2020). One such example are Rubiscos from

328 C_4 species. Rubisco from C_4 species have greater k_{cat} and K_c values compared to C_3 species

329 and there is variation amongst C_4 species of different decarboxylation types (Ghannoum et

330 al., 2005; Seemann et al., 1984; Sharwood et al., 2016a; Yeoh et al., 1980). Superior k_{cat} in C_4

331 grasses of the NADP-ME biochemical subtype compared to C_4 grasses with the NAD-ME

332 decarboxylation subtypes resulted in better N use efficiency in NADP-ME compared to NAD-

333 ME subtypes (Ghannoum et al., 2005). Rubisco from C_4 species are excellent candidates for

334 transplanting into C_3 species (Sharwood et al., 2016a; Sharwood et al., 2016b). For more

335 information on variation in Rubisco kinetic properties see Tcherkez et al. (2006) and

336 Flamholz et al. (2019).

337 Whitney and collaborators have used plastid transformation in tobacco to manipulate

338 Rubisco the large subunit (Whitney and Andrews, 2001a, b; Whitney et al., 1999). They

339 showed that the differences between the C_3 and C_4 forms of Rubisco from Flaveria species

340 could be largely explained by a single amino acid change between Met-309 (C_3 type with

341 lower K_c and k_{cat}) and Ile-309 (C_4 type with higher K_c and k_{cat}) highlighting the potential of

342 large subunit manipulation. Rubisco from no-green algae such as *Griffithsia monilis* have a

343 higher specificity for CO_2 coupled with lower K_c for CO_2 at ambient O_2 also make excellent

344 candidates but to date the assembly in tobacco chloroplasts has not been successful (Lin

345 and Hanson, 2018; Whitney et al., 2001). Furthermore chloroplast transformation is only

346 possible in a few species limiting the scope at present (Bock, 2015).

347 In C_3 species, Rubisco operates in a low CO_2 environment, which is suboptimal for both

348 catalysis and carbamylation of the active sites (for review see von Caemmerer, 2000). The

349 activation of Rubisco *in vivo* requires the presence of the regulatory protein Rubisco activase

350 (Mate et al., 1996; Portis, 2003; Portis et al., 1986). Rubisco activase aids the release of

351 sugar phosphate inhibitors from Rubisco's catalytic sites, thereby influencing carbamylation.

352 Rubisco activase is an AAA+ ATPase which uses the energy from the hydrolysis of ATP to

353 release inhibitors from Rubiscos catalytic sites. Rubisco is typically fully activated to 80-90%

354 at high light except at high temperatures (Crafts-Brandner and Salvucci, 2000; Scafaro et al.,

355 2012; Sharwood et al., 2016c; von Caemmerer and Edmondson, 1986; Yamori et al., 2006).

356 There are two main reasons why the Rubisco/Rubisco activase interaction is a target for

357 crop improvement. It is thought that inactivation of CO_2 assimilation by heat stress, which is

358   of great agricultural significance, is caused by inactivation of Rubisco activase at high

359   temperature. Secondly the slow rate of photosynthetic light induction is due to slow

360   Rubisco activation (Carmo-Silva and Salvucci, 2013; Parry et al., 2013; Taylor and Long,

361   2017). Two separate studies in Arabidopsis demonstrated that replacing the native Rubisco

362   activase with a more thermostable form increased plant tolerance to heat stress (Kumar et

363   al., 2009; Kurek et al., 2007). Over expression of a thermally stable Rubisco activase from a

364   wild relative *Oryza australiensis* in a domesticated rice (Oryza sativa) was also shown to

365   improve seed yield (Scafaro et al., 2018). Now, conserved sequence identified in Rubisco

366   activase from heat-adapted species has been shown to improves wheat Rubisco activase

367   thermo-stability in vitro (Degen et al., 2020; Scafaro et al., 2019). New, more thermally

368   stable forms of activase are being identified and structural information for Rubisco activase

369   is providing key information towards understanding of how the two enzymes interact

370   (Mueller-Cajar et al., 2014; Shivhare and Mueller-Cajar, 2017; Shivhare et al., 2019).

371   Rubisco activase has two major isforms (α and β) that exist in higher plant species, with the

372   longer α isoform redox-regulated and influencing the rate of increase in CO_2 fixation in a

373   dark to light transition. Induction being much more rapid in transgenic plants expressing

374   only the shorter isoform (Carmo-Silva and Salvucci, 2013; Carmo-Silva et al., 2015). The

375   effect on the rate of photosynthetic induction was also demonstrated in tobacco transgenic

376   with an antisense construct to Rubisco activase (Hammond et al., 1995). Overexpression of

377   Rubisco activase leads to an increase in the rate light induction (Fukayama et al., 2012;

378   Yamori et al., 2012). However it is curious to note that overexpression of Rubisco activase

379   can decrease steady state CO_2 assimilation rate by reducing Rubisco content (Fukayama et

380   al., 2012; Suganami et al., 2020). The parallel of increased Rubisco content in Rubisco

381   antisense plant has been observed in both tobacco and rice and speaks of a curious link

382   between Rubisco and Rubisco activase synthesis (He et al., 1997).

383   **Conclusion**

384   The discovery of Rubiscos oxygenase function has led to the developments of our current

385   mathematical models of CO_2 assimilation. Linking the in vitro kinetic parameters of Rubisco

386   to in vivo gas exchange remains crucial for both terrestrial biosphere and crop models and

387   provides a guide for identifying targets for improving photosynthetic CO_2 assimilation and

388   crop growth. New technological advances such as hyperspectral reflectance measurements

389   are providing better time resolved measurements of Rubisco capacity in the biosphere and

390   these techniques are proving equally important in monitoring seasonal variation in crop

391   photosynthesis. At present we know little about what dictates variation in Rubisco and

392   photosynthetic capacity in variable environments and more needs to be learned about

393   these signal transduction pathways.

398

399

Figures

Figure 1

a) Modelled oxygen dependence of the CO_2 compensation point in the presence of mitochondrial respiration, Γ (equation 6) or the absence of mitochondrial respiration, Γ_* (equation 5).

b) Modelled response of CO_2 assimilation rate, A versus chloroplast CO_2 partial pressure, C at 200 and 20 mbar O_2. The figure is adapted from von Caemmerer (2000) using equations 2.2 and 2.23 and kinetic constants from table 2.3, with V_{cmax}= 80 µmol m^{-2} s^{-1}, J=132 µmol m^{-2} s^{-1} and R_d =1 µmol m^{-2} s^{-1}.

Figure 2

The stoichiometry of the photosynthetic carbon reduction (PCR) cycle and the photorespiratory carbon oxidation (PCO) cycle. Note that the regeneration of 0.5 mol of PGA from 1 mol PGly requires the 0.5 mol ATP. It also includes the release and refixation 0.5 mol of ammonia which requires 1 mol of reduced ferredoxin which in terms of electron transport is equivalent to 0.5 mol of NADPH and 0.5 mol of ATP (Keys et al., 1978) The stoichiometry and diagram are adapted from Farquhar et al. (1980).

Figure 3

Monthly averages of atmospheric CO_2 (a) and the carbon isotope composition of atmospheric CO_2 (b) sampled in flasks at Mauna Loa, Hawaii. Data were downloaded from www.cmdl.noaa.gov (Dlugokencky et al., 2019; White et al., 2018). The figure illustrates the rising atmospheric CO_2 concentration together with the inter-annual oscillation. Increased photosynthesis in the summer months results in a decrease in atmospheric CO_2. Rubisco's action is apparent in (b) from the increase in $\delta^{13}C$ which indicates an increase $^{13}CO_2$ in the atmosphere as Rubisco preferentially fixes $^{12}CO_2$. ($\delta^{13}C$ is defined as $\frac{^{13}C}{^{12}C}air \bigg/ \frac{^{13}C}{^{12}C}std - 1$, where the standard it PBD belemnite (Farquhar et al., 1989)).

Figure 4

427   Modelled response of CO_2 assimilation rate, A versus chloroplast (C_3) or mesophyll (C_4) CO_2

428   partial pressure, C at 200 mbar O_2. For C_3 photosynthesis the model uses equations 9 and

429   11 with K_C=260 µbar K_O=179 mbar and Γ*= 38.6 µbar. V_{cmax}= 80 µmol m^{-2} s^{-1} and J=132 µmol

430   m^{-2} s^{-1} and R_d =1 µmol m^{-2} s^{-1}. The Rubisco kinetic constants for the red algal Rubisco

431   (*Griffithsia monilis*) were taken from Fig. 4 (Sharwood, 2017). Expressed in the gaseous

432   phase K_C=278 µbar K_O=563 mbar and Γ*= 22.6 µbar. V_{cmax}= 67 µmol m^{-2} s^{-1} and J=132 µmol

433   m^{-2} s^{-1} and R_d =1 µmol m^{-2} s^{-1}. The V_{cmax} is lower to keep the same Rubisco site content for

434   both C_3 curves of 25.8 µmol m^{-2}. The A-C curve for C_4 photosynthesis uses the model

435   equations from von Caemmerer (2000) together with the PEP carboxylase and Rubisco

436   kinetic constants from *Setaria viridis* (Boyd et al., 2015). K_C=1210 µbar K_O=292 mbar and Γ*=

437   76.3 µbar. V_{cmax}= 40 µmol m^{-2} s^{-1} and the PEP carboxylase parameters are V_{pmax}= 300 µmol

438   m^{-2} s^{-1}, The K_m CO_2 for PEPC, K_p=154 µbar and a bundle sheath conductance to CO_2 of 3

439   mmol m^{-1} s^{-1} bar^{-1} (Alonso-Cantabrana et al., 2018). Note that a V_{cmax}= 40 µmol m^{-2} s^{-1}

440   corresponds to a Rubisco site content of 7.35 µmol m^{-2}.

441

References

443   Aigner, H., Wilson, R.H., Bracher, A., Calisse, L., Bhat, J.Y., Hartl, F.U., Hayer-Hartl, M., 2017.
444   Plant RuBisCo assembly in *E. coli* with five chloroplast chaperones including BSD2. Science
445   358(6368), 1272-1278.

446   Alonso-Cantabrana, H., Cousins, A.B., Danila, F., Ryan, T., Sharwood, R.E., von Caemmerer,
447   S., Furbank, R.T., 2018. Diffusion of CO_2 across the mesophyll-bundle sheath cell interface in
448   a C_4 plant with genetically reduced PEP carboxylase activity. Plant Physiology 178(1), 72-81.

449   Alton, P.B., 2017. Retrieval of seasonal Rubisco-limited photosynthetic capacity at global
450   FLUXNET sites from hyperspectral satellite remote sensing: Impact on carbon modelling.
451   Agricultural and Forest Meteorology 232, 74-88.

452   Andersson, I., Backlund, A., 2008. Structure and function of Rubisco. Plant Physiology and
453   Biochemistry 46(3), 275-291.

454   Andrews, T.J., Lorimer, G.H., 1987. Rubisco: Structure, mechanisms, and prospects for
455   improvement, in: Hatch, M.D., Boardman, N.K. (Eds.), The Biochemistry of Plants: A
456   Comprehensive Treatise. Vol 10, Photosynthesis. Academic Press, New York, pp. 131-218.

457   Ashida, H., Saito, Y., Nakano, T., Tandeau de Marsac, N., Sekowska, A., Danchin, A., Yokota,
458   A., 2008. RuBisCO-like proteins as the enolase enzyme in the methionine salvage pathway:
459   functional and evolutionary relationships between RuBisCO-like proteins and
460   photosynthetic RuBisCO. Journal of Experimental Botany 59(7), 1543-1554.

461 Atkin, O.K., Evans, J.R., Ball, M.C., Lambers, H., Pons, T.L., 2000. Leaf Respiration of Snow
462 Gum in the Light and Dark. Interactions between Temperature and Irradiance. Plant
463 Physiology 122(3), 915-924.

464 Badger, M.R., Andrews, T.J., 1974. Effects of CO_2, O_2 and temperature on a high-affinity
465 form of ribulose diphosphate carboxylase-oxygenase from spinach. Biochemical and
466 Biophysical Research Communications 60(1), 204-210.

467 Badger, M.R., Andrews, T.J., Whitney, S.M., Ludwig, M., Yellowlees, D.C., Leggat, W., Price,
468 G.D., 1998. The diversity and coevolution of rubisco, plastids, pyrenoids, and chloroplast-
469 based CO_2-concentrating mechanisms in algae. Canadian Journal of Botany-Revue
470 Canadienne de Botanique 76(6), 1052-1071.

471 Badger, M.R., Collatz, G.J., 1977. Studies on the kinetic mechanism of RuBP carboxylase and
472 oxygenase reactions, with particular reference to the effect of temperature on kinetic
473 papameters. Carnegie Institute of Washington Yearbook 76, 355-361.

474 Badger, M.R., Sharkey, T.D., von Caemmerer, S., 1984. The relationship between steady-
475 state gas exchange of bean leaves and the levels of carbon-reduction cycle intermediates.
476 Planta 160, 305-313.

477 Bailey-Serres, J., Parker, J.E., Ainsworth, E.A., Oldroyd, G.E.D., Schroeder, J.I., 2019. Genetic
478 strategies for improving crop yields. Nature 575(7781), 109-118.

479 Bar-On, Y.M., Milo, R., 2019. The global mass and average rate of rubisco. Proceedings of
480 the National Academy of Sciences 116(10), 4738-4743.

481 Bernacchi, C.J., Bagley, J.E., Serbin, S.P., Ruiz-Vera, U.M., Rosenthal, D.M., Vanloocke, A.,
482 2013. Modelling C_3 photosynthesis from the chloroplast to the ecosystem. Plant Cell and
483 Environment 36(9), 1641-1657.

484 Bernacchi, C.J., Portis, A.R., Nakano, H., von Caemmerer, S., Long, S.P., 2002. Temperature
485 response of mesophyll conductance. Implications for the determination of Rubisco enzyme
486 kinetics and for limitations to photosynthesis in vivo. Plant Physiology 130(4), 1992-1998.

487 Björkman, O., 1968. Carboxydismutase activity in shade and sun adapted species of higher
488 plants. Physiol.Plantarum 21, 1-10.

489 Bock, R., 2015. Engineering Plastid Genomes: Methods, Tools, and Applications in Basic
490 Research and Biotechnology. Annual Review of Plant Biology 66(1), 211-241.

491 Bowes, G., Ogren, W.L., 1972. Oxygen inhibition and other properties of soybean RuDP
492 carboxylase. J. Biol. Chem 247, 2171-2176.

493 Bowes, G., Ogren, W.L., Hageman, R.H., 1971. Phosphoglycolate production catalyzed by
494 ribulose diphosphate carboxylase. Biochemical and Biophysical Research Communications
495 45, 716-722.

496 Boyd, R.A., Cavanagh, A.P., Kubien, D.S., Cousins, A.B., 2018. Temperature response of
497 Rubisco kinetics in Arabidopsis thaliana: thermal breakpoints and implications for reaction
498 mechanisms. Journal of Experimental Botany 70(1), 231-242.

499 Boyd, R.A., Gandin, A., Cousins, A.B., 2015. Temperature responses of C_4 photosynthesis:
500 Biochemical analysis of Rubisco, Phosphoenolpyruvate Carboxylase, and Carbonic
501 Anhydrase in *Setaria viridis*. Plant Physiology 169(3), 1850-1861.

502 Bracher, A., Whitney, S.M., Hartl, F.U., Hayer-Hartl, M., 2017. Biogenesis and Metabolic
503 Maintenance of Rubisco. Annual Review of Plant Biology 68(1), 29-60.

504 Brooks, A., Farquhar, G.D., 1985. Effect of temperature on the CO_2/O_2 specificity of ribulose-
505 1,5-bisphosphate carboxylase oxygenase and the rate of respiration in the light - estimates
506 from gas-exchange measurements on spinach. Planta 165, 397-406.

507 Busch, F.A., 2020. Photorespiration in the context of Rubisco biochemistry, CO2 diffusion
508 and metabolism. The Plant Journal 101(4), 919-939.

509 Busch, F.A., Sage, R.F., Farquhar, G.D., 2018. Plants increase CO_2 uptake by assimilating
510 nitrogen via the photorespiratory pathway. Nature Plants 4(1), 46-54.

511 Carmo-Silva, A.E., Salvucci, M.E., 2013. The Regulatory Properties of Rubisco Activase Differ
512 among Species and Affect Photosynthetic Induction during Light Transitions. Plant
513 Physiology 161(4), 1645-1655.

514 Carmo-Silva, E., Scales, J.C., Madgwick, P.J., Parry, M.A.J., 2015. Optimizing Rubisco and its
515 regulation for greater resource use efficiency. Plant Cell and Environment 38(9), 1817-1832.

516 Cousins, A.B., Ghannoum, O., von Caemmerer, S., Badger, M.R., 2010. Simultaneous
517 determination of Rubisco carboxylase and oxygenase kinetic parameters in Triticum
518 aestivum and Zea mays using membrane inlet mass spectrometry. Plant Cell and
519 Environment 33(3), 444-452.

520 Cousins, A.B., Pracharoenwattana, I., Zhou, W.X., Smith, S.M., Badger, M.R., 2008.
521 Peroxisomal malate dehydrogenase is not essential for photorespiration in Arabidopsis but
522 its absence causes an increase in the stoichiometry of photorespiratory CO_2 release. Plant
523 Physiology 148(2), 786-795.

524 Cousins, A.B., Walker, B.J., Pracharoenwattana, I., Smith, S.M., Badger, M.R., 2011.
525 Peroxisomal hydroxypyruvate reductase is not essential for photorespiration in Arabidopsis
526 but its absence causes an increase in the stoichiometry of photorespiratory CO_2 release.
527 Photosynthesis Research 108(2-3), 91-100.

528 Crafts-Brandner, S.J., Salvucci, M.E., 2000. Rubisco activase constrains the photosynthetic
529 potential of leaves at high temperature and CO_2. Proceedings of the National Academy of
530 Sciences of the United States of America 97(24), 13430-13435.

531 Dechant, B., Cuntz, M., Vohland, M., Schulz, E., Doktor, D., 2017. Estimation of
532 photosynthesis traits from leaf reflectance spectra: Correlation to nitrogen content as the
533 dominant mechanism. Remote Sensing of Environment 196, 279-292.

534 Degen, G.E., Worrall, D., Carmo-Silva, E., 2020. An isoleucine residue acts as a thermal and
535 regulatory switch in wheat Rubisco activase. The Plant Journal n/a(n/a).

536 Dlugokencky, E.J., Mund, J.W., Crotwell, A.M., Crotwell, M.J., Thoning, K.W., 2019.
537 Atmospheric Carbon Dioxide Dry Air Mole Fractions from the NOAA ESRL Carbon Cycle
538 Cooperative Global Air Sampling Network, 1968-2018, Version: 2019-07.
539 https://doi.org/10.15138/wkgj-f215.

540 Ehleringer, J., Björkman, O., 1976. Quantum yield and temperature dependence of the
541 quantum yield for CO2 uptake in C_3 and C_4 plants. Carnegie YB 75, 418-421.

542 Ellis, R.J., 1979. The most abundant protein in the world. Trends in Biochemical Sciences 4,
543 241-244.

544 Ermakova, M., Danila, F.R., Furbank, R.T., von Caemmerer, S., 2020. On the road to C4 rice:
545 advances and perspectives. The Plant Journal 101(4), 940-950.

546 Evans, J.R., 2013. Improving Photosynthesis. Plant Physiology 162(4), 1780-1793.

547 Evans, J.R., Clarke, V.C., 2018. The nitrogen cost of photosynthesis. Journal of Experimental
548 Botany 70(1), 7-15.

549 Farquhar, G.D., 1979. Models describing the kinetics of RuBP carboxylase-oxygenase.
550 Archives of Biochemistry and Biophysics 193, 456-468.

551 Farquhar, G.D., Ehleringer, J.R., Hubick, K.T., 1989. Carbon isotope discrimination and
552 photosynthesis. Annual Review of Plant Physiology and Plant Molecular Biology 40, 503-537.

553 Farquhar, G.D., von Caemmerer, S., 1982. Modelling of photosynthetic response to
554 environmental conditions, in: Lange, O.L., Nobel, P.S., Osmond, C.B., Ziegler, H. (Eds.),
555 Physiological Plant Ecology II. Encyclopedia of Plant Physiology, New Series, Vol. 12 B.
556 Springer Verlag, Berlin Heidelberg, pp. 550-587.

557 Farquhar, G.D., von Caemmerer, S., Berry, J.A., 1980. A biochemical-model of
558 photosynthetic CO_2 assimilation in leaves of C_3 species. Planta 149, 78-90.

559 Flamholz, A.I., Prywes, N., Moran, U., Davidi, D., Bar-On, Y.M., Oltrogge, L.M., Alves, R.,
560 Savage, D., Milo, R., 2019. Revisiting Trade-offs between Rubisco Kinetic Parameters.
561 Biochemistry 58(31), 3365-3376.

562 Flexas, J., Barbour, M.M., Brendel, O., Cabrera, H.M., Carriqui, M., Diaz-Espejo, A., Douthe,
563 C., Dreyer, E., Ferrio, J.P., Gago, J., Galle, A., Galmes, J., Kodama, N., Medrano, H., Niinemets,
564 U., Peguero-Pina, J.J., Pou, A., Ribas-Carbo, M., Tomas, M., Tosens, T., Warren, C.R., 2012.
565 Mesophyll diffusion conductance to CO_2: An unappreciated central player in photosynthesis.
566 Plant Science 193, 70-84.

567   Forrester, M.L., Krotkov, G., Nelson, C.D., 1966. Effect of Oxygen on Photosynthesis,
568   Photorespiration and Respiration in Detached Leaves. I. Soybean. Plant Physiology 41(3),
569   422-427.

570   Fukayama, H., Ueguchi, C., Nishikawa, K., Katoh, N., Ishikawa, C., Masumoto, C., Hatanaka,
571   T., Misoo, S., 2012. Overexpression of Rubisco Activase Decreases the Photosynthetic CO_2
572   Assimilation Rate by Reducing Rubisco Content in Rice Leaves. Plant and Cell Physiology
573   53(6), 976-986.

574   Furbank, R.T., Sharwood, R., Estavillo, G.M., Silva-Perez, V., Condon, A.G., 2020. Photons to
575   food: genetic improvement of cereal crop photosynthesis. Journal of Experimental Botany.

576   Gago, J., Carriquí, M., Nadal, M., Clemente-Moreno, M.J., Coopman, R.E., Fernie, A.R.,
577   Flexas, J., 2019. Photosynthesis optimized across land plant phylogeny. Trends in Plant
578   Science 24(10), 947-958.

579   Galmés, J., Hermida-Carrera, C., Laanisto, L., Niinemets, Ü., 2016. A compendium of
580   temperature responses of Rubisco kinetic traits: variability among and within
581   photosynthetic groups and impacts on photosynthesis modeling. Journal of Experimental
582   Botany 67(17), 5067-5091.

583   Ghannoum, O., Evans, J.R., Chow, W.S., Andrews, T.J., Conroy, J.P., von Caemmerer, S.,
584   2005. Faster rubisco is the key to superior nitrogen-use efficiency in NADP-malic enzyme
585   relative to NAD-malic enzyme C_4 grasses. Plant Physiology 137(2), 638-650.

586   Hall, A., Björkman, O., 1975. A model of leaf photosynthesis and respiration, in: Gates, D.M.,
587   Schmerl, R. (Eds.), Perspectives of biophysical ecology. Springer, Berlin, pp. 55-72.

588   Hall, A.E., 1979. A model of leaf photosynthesis and respiration for predicting carbon dioxide
589   assimilation in different environments. Oecologia 143, 299-316.

590   Hammond, E.T., Hudson, G.S., Andrews, T.J., Woodrow, I.E., 1995. Analysis of Rubisco
591   activation using tobacco with anti-sense RNA to Rubisco activase, in: Mathis, P. (Ed.)
592   Photosynthesis: from Light to Biosphere. Kluwer Academic Publishers, Dordrecht, pp. 293-
593   296.

594   Hanson, K.R., Peterson, R.B., 1986. Regulation of photorespiration in leaves: Evidence that
595   the fraction of ribulose bisphosphate oxygenated is conserved and stoichiometry fluctuates.
596   Archives of Biochemistry and Biophysics 246, 332-346.

597   Harley, P.C., Sharkey, T.D., 1991. An improved model of C_3 photosynthesis at high CO_2:
598   Reversed O_2 sensitivity explained by lack of glycerate reentry into the chloroplast.
599   Photosynthesis Research 27, 169-178.

600   Hayer-Hartl, M., 2020. Cellular Machineries Devoted to Rubisco – the Most Abundant
601   Enzyme. The FASEB Journal 34(S1), 1-1.

602   He, Z., von Caemmerer, S., Hudson, G.S., Price, G.D., Badger, M.R., Andrews, T.J., 1997.
603   Ribulose-1,5-bisphosphate carboxylase/oxygenase activase deficiency delays senescence of

604 ribulose-1,5-bisphosphate carboxylase/oxygenase but progressively impairs its catalysis
605 during tobacco leaf development. Plant Physiology 115, 1569-1580.

606 Hennacy, J.H., Jonikas, M.C., 2020. Prospects for Engineering Biophysical CO_2 Concentrating
607 Mechanisms into Land Plants to Enhance Yields. Annual Review of Plant Biology 71(1), null.

608 Iñiguez, C., Capó-Bauçà, S., Niinemets, Ü., Stoll, H., Aguiló-Nicolau, P., Galmés, J., 2020.
609 Evolutionary trends in RuBisCO kinetics and their co-evolution with CO_2 concentrating
610 mechanisms. The Plant Journal 101(4), 897-918.

611 Jensen, R.G., Bahr, J.T., 1977. Ribulose 1,5-bisphosphate carboxylase-oxygenase. Annual
612 Review of Plant Physiology and Plant Molecular Biology 28, 379-400.

613 Jordan, D.B., Ogren, W.L., 1981. Species variation in the specificity of ribulose bisphosphate
614 carboxylase/oxygenase. Nature 291, 513-515.

615 Kattge, J., Knorr, W., 2007. Temperature acclimation in a biochemical model of
616 photosynthesis: a reanalysis of data from 36 species. Plant Cell Environ 30(9), 1176-1190.

617 Kattge, J., Knorr, W., Raddatz, T., Wirth, C., 2009. Quantifying photosynthetic capacity and
618 its relationship to leaf nitrogen content for global-scale terrestrial biosphere models. Global
619 Change Biology 15(4), 976-991.

620 Kebeish, R., Niessen, M., Thiruveedhi, K., Bari, R., Hirsch, H.J., Rosenkranz, R., Stabler, N.,
621 Schonfeld, B., Kreuzaler, F., Peterhansel, C., 2007. Chloroplastic photorespiratory bypass
622 increases photosynthesis and biomass production in *Arabidopsis thaliana*. Nat Biotechnol
623 25(5), 593-599.

624 Keys, A.J., Bird, I.F., Cornelius, M.J., Lea, P.J., Wallsgrove, R.M., Miflin, B.J., 1978.
625 Photorespiratory nitrogen cycle. Nature 275, 741-743.

626 Knauer, J., Zaehle, S., De Kauwe, M.G., Haverd, V., Reichstein, M., Sun, Y., 2020. Mesophyll
627 conductance in land surface models: effects on photosynthesis and transpiration. The Plant
628 Journal 101(4), 858-873.

629 Kumar, A., Li, C.S., Portis, A.R., 2009. Arabidopsis thaliana expressing a thermostable
630 chimeric Rubisco activase exhibits enhanced growth and higher rates of photosynthesis at
631 moderately high temperatures. Photosynthesis Research 100(3), 143-153.

632 Kurek, I., Chang, T.K., Bertain, S.M., Madrigal, A., Liu, L., Lassner, M.W., Zhu, G.H., 2007.
633 Enhanced thermostability of Arabidopsis Rubisco activase improves photosynthesis and
634 growth rates under moderate heat stress. Plant Cell 19(10), 3230-3241.

635 Laing, W.A., Ogren, W.L., Hageman, R.H., 1974. Regulation of soybean net photosynthetic
636 CO_2 fixation by the interaction of CO_2, O_2, and ribulose 1,5-bisphosphate carboxylase. Plant
637 Physiology 54, 678-685.

638 Laisk, A., 1970. A model of leaf photosynthesis and photorespiration, Prediction and
639 measurement of photosynthetic productivity. Proc IBP/PP Tech Meet Trebon 1969,
640 Wageningen, pp. 295-306.

641 Laisk, A., 1977. Kinetics of photosynthesis and photorespiration in C_3 plants. Nauka,
642 Moscow.

643 Lin, M.T., Hanson, M.R., 2018. Red algal Rubisco fails to accumulate in transplastomic
644 tobacco expressing Griffithsia monilis RbcL and RbcS genes. Plant Direct 2(2), e00045.

645 Liu, C., Young, A.L., Starling-Windhof, A., Bracher, A., Saschenbrecker, S., Rao, B.V., Rao, K.V.,
646 Berninghausen, O., Mielke, T., Hartl, F.U., Beckmann, R., Hayer-Hartl, M., 2010. Coupled
647 chaperone action in folding and assembly of hexadecameric Rubisco. Nature 463(7278),
648 197-202.

649 Long, B.M., Hee, W.Y., Sharwood, R.E., Rae, B.D., Kaines, S., Lim, Y.-L., Nguyen, N.D., Massey,
650 B., Bala, S., von Caemmerer, S., Badger, M.R., Price, G.D., 2018. Carboxysome encapsulation
651 of the CO2-fixing enzyme Rubisco in tobacco chloroplasts. Nat. Commun 9(1), 3570.

652 Long, S.P., Zhu, X.G., Naidu, S.L., Ort, D.R., 2006. Can improvement in photosynthesis
653 increase crop yields? Plant Cell and Environment 29(3), 315-330.

654 Lorimer, G.H., Badger, M.R., Andrews, T.J., 1976. The activation of ribulose-1,5-
655 bisphosphate carboxylase by carbon dioxide and magnesium ions. Equilibria, kinetics, a
656 suggested mechanism and physiological implications. Biochemistry 15, 529-536.

657 Mate, C.J., von Caemmerer, S., Evans, J.R., Hudson, G.S., Andrews, T.J., 1996. The
658 relationship between CO_2-assimilation rate, Rubisco carbamylation and Rubisco activase
659 content in activase-deficient transgenic tobacco suggests a simple model of activase action.
660 Planta 198(4), 604-613.

661 Meacham-Hensold, K., Fu, P., Wu, J., Serbin, S., Montes, C.M., Ainsworth, E., Guan, K.,
662 Dracup, E., Pederson, T., Driever, S., Bernacchi, C., 2020. Plot-level rapid screening for
663 photosynthetic parameters using proximal hyperspectral imaging. Journal of Experimental
664 Botany 71(7), 2312-2328.

665 Meacham-Hensold, K., Montes, C.M., Wu, J., Guan, K., Fu, P., Ainsworth, E.A., Pederson, T.,
666 Moore, C.E., Brown, K.L., Raines, C., Bernacchi, C.J., 2019. High-throughput field
667 phenotyping using hyperspectral reflectance and partial least squares regression (PLSR)
668 reveals genetic modifications to photosynthetic capacity. Remote Sensing of Environment
669 231, 111176.

670 Miyazawa, S.-I., Tobita, H., Ujino-Ihara, T., Suzuki, Y., 2020. Oxygen response of leaf CO2
671 compensation points used to determine Rubisco specificity factors of gymnosperm species.
672 J. Plant Res 133(2), 205-215.

673 Mueller-Cajar, O., Stotz, M., Bracher, A., 2014. Maintaining photosynthetic CO2 fixation via
674 protein remodelling: the Rubisco activases. Photosynthesis Research 119(1-2), 191-201.

675   O'Leary, M.H., 1981. Carbon isotope fractionations in plants Phytochemistry 20, 553-567.

676   Ogren, W.L., 2003. Affixing the O to Rubisco : discovering the source of photorespiratory
677   glycolate and its regulation. Photosynthesis Research 76(1-3), 53-63.

678   Orr, D.J., Alcântara, A., Kapralov, M.V., Andralojc, P.J., Carmo-Silva, E., Parry, M.A.J., 2016.
679   Surveying Rubisco Diversity and Temperature Response to Improve Crop Photosynthetic
680   Efficiency. Plant Physiology 172(2), 707-717.

681   Ort, D.R., Merchant, S.S., Alric, J., Barkan, A., Blankenship, R.E., Bock, R., Croce, R., Hanson,
682   M.R., Hibberd, J.M., Long, S.P., Moore, T.A., Moroney, J., Niyogi, K.K., Parry, M.A.J., Peralta-
683   Yahya, P.P., Prince, R.C., Redding, K.E., Spalding, M.H., van Wijk, K.J., Vermaas, W.F.J., von
684   Caemmerer, S., Weber, A.P.M., Yeates, T.O., Yuan, J.S., Zhu, X.G., 2015. Redesigning
685   photosynthesis to sustainably meet global food and bioenergy demand. Proceedings of the
686   National Academy of Sciences of the United States of America 112(28), 8529-8536.

687   Parry, M.A.J., Andralojc, P.J., Scales, J.C., Salvucci, M.E., Carmo-Silva, A.E., Alonso, H.,
688   Whitney, S.M., 2013. Rubisco activity and regulation as targets for crop improvement.
689   Journal of Experimental Botany 64(3), 717-730.

690   Parry, M.A.J., Madgwick, P.J., Carvalho, J.F.C., Andralojc, P.J., 2007. Prospects for increasing
691   photosynthesis by overcoming the limitations of Rubisco. Journal of Agricultural Science
692   145, 31-43.

693   Peguero-Pina, J.J., Flexas, J., Galmes, J., Niinemets, U., Sancho-Knapik, D., Barredo, G.,
694   Villarroya, D., Gil-Pelegrin, E., 2012. Leaf anatomical properties in relation to differences in
695   mesophyll conductance to CO_2 and photosynthesis in two related Mediterranean Abies
696   species. Plant Cell and Environment 35(12), 2121-2129.

697   Peisker, M., 1974. A model describing the influence of oxygen on photosynthetic
698   carboxylation. Photosynthetica 8, 47-50.

699   Peisker, M., Ticha, I., Catsky, J., 1981. Ontogentic changes in the internal limitations to bean
700   leaf photosynthesis. 7. Interpretations of the linear correlation between CO_2 compensation
701   concentration and CO_2 evolution in darkness. Photosynthetica 15, 161-168.

702   Portis, A.R., 2003. Rubisco activase - Rubisco's catalytic chaperone. Photosynthesis Research
703   75(1), 11-27.

704   Portis, A.R., Jr., Salvucci, M.E., Ogren, W.L., 1986. Activation of ribulose bisphosphate
705   carboxylase/oxygenase at physiological CO_2 and ribulosebisphosphate concentrations by
706   rubisco activase. Plant Physiology 82, 967-971.

707   Portis, A.R., Parry, M.A.J., 2007. Discoveries in Rubisco (Ribulose 1,5-bisphosphate
708   carboxylase/oxygenase): a historical perspective. Photosynthesis Research 94(1), 121-143.

709   Portis Jr, A.R., Salvucci, M.E., 2002. The discovery of Rubisco activase – yet another story of
710   serendipity. Photosynthesis Research 73(1), 257-264.

711   Raven, J.A., 2013. Rubisco: still the most abundant protein of Earth? New Phytologist 198(1),
712   1-3.

713   Ray, D.K., Mueller, N.D., West, P.C., Foley, J.A., 2013. Yield Trends Are Insufficient to Double
714   Global Crop Production by 2050. Plos One 8(6), e66428.

715   Rogers, A., Medlyn, B.E., Dukes, J.S., Bonan, G., von Caemmerer, S., Dietze, M.C., Kattge, J.,
716   Leakey, A.D.B., Mercado, L.M., Niinemets, Ü., Prentice, I.C., Serbin, S.P., Sitch, S., Way, D.A.,
717   Zaehle, S., 2017. A roadmap for improving the representation of photosynthesis in Earth
718   system models. New Phytologist 213(1), 22-42.

719   Roy, H., Andrews, T.J., 2000. Rubisco: assembly and mechanism., in: Leegood, R.C., Sharkey,
720   T.D., von Caemmerer, S. (Eds.), Photosynthesis - Physiology and Metabolism. Kluwever
721   Academic Publishers, The Netherlands, pp. 53-83.

722   Salesse-Smith, C.E., Sharwood, R.E., Busch, F.A., Kromdijk, J., Bardal, V., Stern, D.B., 2018.
723   Overexpression of Rubisco subunits with RAF1 increases Rubisco content in maize. Nature
724   Plants 4(10), 802-810.

725   Salesse-Smith, C.E., Sharwood, R.E., Busch, F.A., Stern, D.B., 2019. Increased Rubisco content
726   in maize mitigates chilling stress and speeds recovery. Plant Biotechnology Journal n/a(n/a).

727   Scafaro, A.P., Atwell, B.J., Muylaert, S., Reusel, B.V., Ruiz, G.A., Rie, J.V., Gallé, A., 2018. A
728   Thermotolerant Variant of Rubisco Activase From a Wild Relative Improves Growth and
729   Seed Yield in Rice Under Heat Stress. Frontiers in Plant Science 9(1663).

730   Scafaro, A.P., Bautsoens, N., den Boer, B., Van Rie, J., Gallé, A., 2019. A Conserved Sequence
731   from Heat-Adapted Species Improves Rubisco Activase Thermostability in Wheat. Plant
732   Physiology 181(1), 43-54.

733   Scafaro, A.P., Yamori, W., Carmo-Silva, A.E., Salvucci, M.E., von Caemmerer, S., Atwell, B.J.,
734   2012. Rubisco activity is associated with photosynthetic thermotolerance in a wild rice
735   (Oryza meridionalis). Physiologia Plantarum 146(1), 99-109.

736   Seemann, J.R., Badger, M.R., Berry, J.A., 1984. Variations in the specific activity of ribulose-
737   1,5-bisphosphate carboxylase between species utilizing differing photosynthetic pathways.
738   Plant Physiology 74, 791-794.

739   Serbin, S.P., Dillaway, D.N., Kruger, E.L., Townsend, P.A., 2012. Leaf optical properties reflect
740   variation in photosynthetic metabolism and its sensitivity to temperature. Journal of
741   Experimental Botany 63(1), 489-502.

742   Serbin, S.P., Singh, A., Desai, A.R., Dubois, S.G., Jablonski, A.D., Kingdon, C.C., Kruger, E.L.,
743   Townsend, P.A., 2015. Remotely estimating photosynthetic capacity, and its response to
744   temperature, in vegetation canopies using imaging spectroscopy. Remote Sensing of
745   Environment 167, 78-87.

746   Sharkey, T.D., 2020. Emerging research in plant photosynthesis. Emerging Topics in Life
747   Sciences.

Sharkey, T.D., Bernacchi, C.J., Farquhar, G.D., Singsaas, E.L., 2007. Fitting photosynthetic carbon dioxide response curves for C_3 leaves. Plant Cell and Environment 30(9), 1035-1040.

Sharwood, R.E., 2017. Engineering chloroplasts to improve Rubisco catalysis: prospects for translating improvements into food and fiber crops. New Phytologist 213(2), 494-510.

Sharwood, R.E., Crous, K.Y., Whitney, S.M., Ellsworth, D.S., Ghannoum, O., 2017. Linking photosynthesis and leaf N allocation under future elevated CO2 and climate warming in Eucalyptus globulus. Journal of Experimental Botany 68(5), 1157-1167.

Sharwood, R.E., Ghannoum, O., Kapralov, M.V., Gunn, L.H., Whitney, S.M., 2016a. Temperature responses of Rubisco from Paniceae grasses provide opportunities for improving C_3 photosynthesis. Nature Plants 2, 16186.

Sharwood, R.E., Ghannoum, O., Whitney, S.M., 2016b. Prospects for improving CO_2 fixation in C_3 crops through understanding C_4 Rubisco biogenesis and catalytic diversity. Current Opinion in Plant Biology 31, 135-142.

Sharwood, R.E., Sonawane, B.V., Ghannoum, O., Whitney, S.M., 2016c. Improved analysis of C_4 and C_3 photosynthesis via refined in vitro assays of their carbon fixation biochemistry. Journal of Experimental Botany 67 3137-3148.

Shivhare, D., Mueller-Cajar, O., 2017. In Vitro Characterization of Thermostable CAM Rubisco Activase Reveals a Rubisco Interacting Surface Loop. Plant Physiology 174(3), 1505-1516.

Shivhare, D., Ng, J., Tsai, Y.-C.C., Mueller-Cajar, O., 2019. Probing the rice Rubisco–Rubisco activase interaction via subunit heterooligomerization. Proceedings of the National Academy of Sciences 116(48), 24041-24048.

Silva-Perez, V., Molero, G., Serbin, S.P., Condon, A.G., Reynolds, M.P., Furbank, R.T., Evans, J.R., 2017. Hyperspectral reflectance as a tool to measure biochemical and physiological traits in wheat. Journal of Experimental Botany 69(3), 483-496.

South, P.F., Cavanagh, A.P., Liu, H.W., Ort, D.R., 2019. Synthetic glycolate metabolism pathways stimulate crop growth and productivity in the field. Science 363(6422), eaat9077.

South, P.F., Cavanagh, A.P., Lopez-Calcagno, P.E., Raines, C.A., Ort, D.R., 2018. Optimizing photorespiration for improved crop productivity. Journal of Integrative Plant Biology 60(12), 1217-1230.

Spreitzer, R.J., Salvucci, M.E., 2002. Rubisco: structure, regulatory interactions, and possibilities for a better enzyme. Annu. Rev. Plant Biol. 53, 449-475.

Stinziano, J.R., Morgan, P.B., Lynch, D.J., Saathoff, A.J., McDermitt, D.K., Hanson, D.T., 2017. The rapid A–Ci response: photosynthesis in the phenomic era. Plant Cell Environ 40(8), 1256-1262.

783 Suganami, M., Suzuki, Y., Kondo, E., Nishida, S., Konno, S., Makino, A., 2020. Effects of
784 Overproduction of Rubisco Activase on Rubisco Content in Transgenic Rice Grown at
785 Different N Levels. International Journal of Molecular Sciences 21(5), 1626.

786 Suits, N.S., Denning, A.S., Berry, J.A., Still, C.J., Kaduk, J., Miller, J.B., Baker, I.T., 2005.
787 Simulation of carbon isotope discrimination of the terrestrial biosphere - art. no. GB1017.
788 Global Biogeochemical Cycles 19(1), B1017.

789 Tabita, F.R., Satagopan, S., Hanson, T.E., Kreel, N.E., Scott, S.S., 2008. Distinct form I, II, III,
790 and IV Rubisco proteins from the three kingdoms of life provide clues about Rubisco
791 evolution and structure/function relationships. Journal of Experimental Botany 59(7), 1515-
792 1524.

793 Taylor, S.H., Long, S.P., 2017. Slow induction of photosynthesis on shade to sun transitions
794 in wheat may cost at least 21% of productivity. Philosophical Transactions of the Royal
795 Society B: Biological Sciences 372(1730), 20160543.

796 Tcherkez, G., 2013. Modelling the reaction mechanism of ribulose-1,5-bisphosphate
797 carboxylase/oxygenase and consequences for kinetic parameters. Plant Cell and
798 Environment 36(9), 1586-1596.

799 Tcherkez, G., 2016. The mechanism of Rubisco-catalysed oxygenation. Plant Cell Environ
800 39(5), 983-997.

801 Tcherkez, G.G.B., Farquhar, G.D., Andrews, T.J., 2006. Despite slow catalysis and confused
802 substrate specificity, all ribulose bisphosphate carboxylases may be nearly perfectly
803 optimized. Proceedings of the National Academy of Sciences of the United States of America
804 103(19), 7246-7251.

805 Timm, S., Hagemann, M., 2020. Photorespiration – how is it regulated and regulates overall
806 plant metabolism? Journal of Experimental Botany.

807 Tregunna, E.B., Downton, J., 1967. Carbon dioxide compensation in members of the
808 Amaranthacea and some related families. Canadian Journal of Botany 45(12), 2385-2387.

809 von Caemmerer, S., 2000. Biochemical models of leaf photosynthesis. CSIRO Publishing,
810 Collingwood, Australia.

811 von Caemmerer, S., 2013. Steady-state models of photosynthesis. Plant Cell Environ 36(9),
812 1617-1630.

813 von Caemmerer, S., Edmondson, D.L., 1986. Relationship between steady-state gas-
814 exchange, *in vivo* ribulose bisphosphate carboxylase activity and some carbon-reduction
815 cycle intermediates in *Raphanus sativus*. Aust J Plant Physiol 13, 669-688.

816 von Caemmerer, S., Evans, J.R., 1991. Determination of the average partial pressure of CO_2
817 in chloroplast from leaves of several C_3 plants. Australian Journal Plant Physiology 18, 287-
818 305.

819   von Caemmerer, S., Evans, J.R., 2015. Temperature responses of mesophyll conductance
820   differ greatly between species. Plant Cell Environ 38(4), 629-637.

821   von Caemmerer, S., Evans, J.R., Hudson, G.S., Andrews, T.J., 1994. The kinetics of ribulose-
822   1,5-bisphosphate carboxylase/oxygenase *in vivo* inferred from measurements of
823   photosynthesis in leaves of transgenic tobacco. Planta 195, 88-97.

824   von Caemmerer, S., Farquhar, G.D., 1981. Some relationships between the biochemistry of
825   photosynthesis and the gas exchange of leaves. Planta 153, 376-387.

826   von Caemmerer, S., Furbank, R.T., 2016. Strategies for improving C 4 photosynthesis.
827   Current opinion in plant biology 31, 125-134.

828   Walker, A.P., Beckerman, A.P., Gu, L., Kattge, J., Cernusak, L.A., Domingues, T.F., Scales, J.C.,
829   Wohlfahrt, G., Wullschleger, S.D., Woodward, F.I., 2014. The relationship of leaf
830   photosynthetic traits – Vcmax and Jmax – to leaf nitrogen, leaf phosphorus, and specific leaf
831   area: a meta-analysis and modeling study. Ecology and Evolution 4(16), 3218-3235.

832   Wareing, P.F., Khalifa, M.M., Treharne, K.J., 1968. Rate-limiting processes in photosynthesis
833   at saturating light intensities. Nature 220, 453-457.

834   White, J.W.C., Vaughn, B.H., Michel, S.E., 2018. Stable Isotopic Composition of Atmospheric
835   Methane (13C) from the NOAA ESRL Carbon Cycle Cooperative Global Air Sampling
836   Network, 1998-2017, Version: 2018-09-24, .
837   ftp://aftp.cmdl.noaa.gov/data/trace_gases/ch4c13/flask/.

838   Whitney, S.M., Andrews, T.J., 2001a. The gene for the ribulose-1,5-bisphosphate
839   carboxylase/oxygenase (Rubisco) small subunit relocated to the plastid genome of tobacco
840   directs the synthesis of small subunits that assemble into Rubisco. Plant Cell 13(1), 193-205.

841   Whitney, S.M., Andrews, T.J., 2001b. Plastome-encoded bacterial ribulose-1,5-bisphosphate
842   carboxylase/oxygenase (RubisCO) supports photosynthesis and growth in tobacco.
843   Proceedings of the National Academy of Sciences of the United States of America 98(25),
844   14738-14743.

845   Whitney, S.M., Baldett, P., Hudson, G.S., Andrews, T.J., 2001. Form I Rubiscos from non-
846   green algae are expressed abundantly but not assembled in tobacco chloroplasts. Plant
847   Journal 26(5), 535-547.

848   Whitney, S.M., Houtz, R.L., Alonso, H., 2011. Advancing our understanding and capacity to
849   engineer nature's CO_2-sequestering enzyme, Rubisco. Plant Physiology 155(1), 27-35.

850   Whitney, S.M., von Caemmerer, S., Hudson, G.S., Andrews, T.J., 1999. Directed mutation of
851   the Rubisco large subunit of tobacco influences photorespiration and growth. Plant
852   Physiology 121(2), 579-588.

853   Wilson, R.H., Thieulin-Pardo, G., Hartl, F.-U., Hayer-Hartl, M., 2019. Improved recombinant
854   expression and purification of functional plant Rubisco. FEBS Lett 593(6), 611-621.

855   Wu, A., Hammer, G.L., Doherty, A., von Caemmerer, S., Farquhar, G.D., 2019. Quantifying
856   impacts of enhancing photosynthesis on crop yield. Nature Plants 5(4), 380-388.

857   Wu, J., Rogers, A., Albert, L.P., Ely, K., Prohaska, N., Wolfe, B.T., Oliveira Jr, R.C., Saleska, S.R.,
858   Serbin, S.P., 2019. Leaf reflectance spectroscopy captures variation in carboxylation capacity
859   across species, canopy environment and leaf age in lowland moist tropical forests. New
860   Phytologist 224(2), 663-674.

861   Wullschleger, S.D., 1993. Biochemical limitations to carbon assimilation in C_3 plants - a
862   retrospective analysis of the A/Ci curves from 109 species. Journal of Experimental Botany
863   44, 907-920.

864   Yamori, W., Evans, J.R., von Caemmerer, S., 2010. Effects of growth and measurement light
865   intensities on temperature dependence of CO_2 assimilation rate in tobacco leaves. Plant Cell
866   and Environment 33(3), 332-343.

867   Yamori, W., Masumoto, C., Fukayama, H., Makino, A., 2012. Rubisco activase is a key
868   regulator of non-steady-state photosynthesis at any leaf temperature and, to a lesser
869   extent, of steady-state photosynthesis at high temperature. Plant Journal 71(6), 871-880.

870   Yamori, W., Nagai, T., Makino, A., 2011. The rate-limiting step for CO_2 assimilation at
871   different temperatures is influenced by the leaf nitrogen content in several C_3 crop species.
872   Plant Cell and Environment 34(5), 764-777.

873   Yamori, W., Suzuki, K., Noguchi, K., Nakai, M., Terashima, I., 2006. Effects of Rubisco kinetics
874   and Rubisco activation state on the temperature dependence of the photosynthetic rate in
875   spinach leaves from contrasting growth temperatures. Plant Cell and Environment 29(8),
876   1659-1670.

877   Yeoh, H.-H., Badger, M.R., Watson, L., 1980. Variations in KM(CO2) of ribulose-1,5-
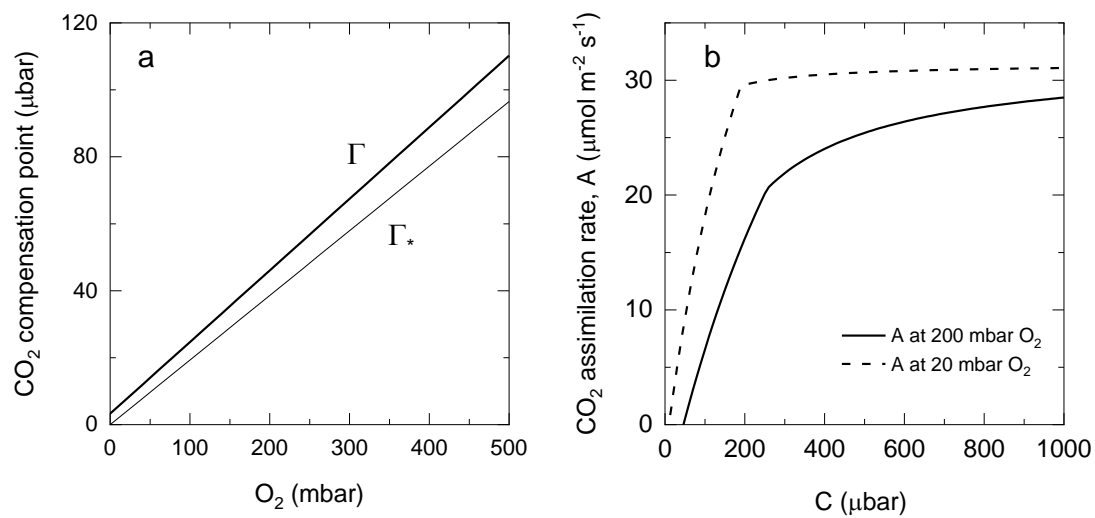878   bisphosphate carboxylase among grasses. Plant Physiology 66, 1110-1112.

879   Yeoh, H.-H., Badger, M.R., Watson, L., 1981. Variations in kinetic-properties of ribulose-1,5-
880   bisphosphate carboxylases among plants. Plant Physiology 67, 1151-1155.

881   Yin, X., Van Oijen, M., Schapendonk, A., 2004. Extension of a biochemical model for the
882   generalized stoichiometry of electron transport limited C_3 photosynthesis. Plant Cell and
883   Environment 27(10), 1211-1222.

884   Yoon, D.-K., Ishiyama, K., Suganami, M., Tazoe, Y., Watanabe, M., Imaruoka, S., Ogura, M.,
885   Ishida, H., Suzuki, Y., Obara, M., Mae, T., Makino, A., 2020. Transgenic rice overproducing
886   Rubisco exhibits increased yields with improved nitrogen-use efficiency in an experimental
887   paddy field. Nature Food 1(2), 134-139.

888   Zelitch, I., 1989. Selection and characterization of tobacco plants with novel O_2-resistant
889   photosynthesis. Plant Physiology 90, 1457-1464.

890   Zhu, X.G., Portis, A.R., Long, S.P., 2004. Would transformation of C_3 crop plants with foreign
891   Rubisco increase productivity? A computational analysis extrapolating from kinetic
892   properties to canopy photosynthesis. Plant Cell and Environment 27(2), 155-165.

893

Figure 1

a) Modelled oxygen dependence of the CO_2 compensation point in the presence of mitochondrial respiration, Γ (equation 6) or the absence of mitochondrial respiration, Γ_* (equation 5).

b) Modelled response of CO_2 assimilation rate, A versus chloroplast CO_2 partial pressure, C at 200 and 20 mbar O_2. The figure is adapted from von Caemmerer (2000) using equations 2.2 and 2.23 and kinetic constants from table 2.3, with V_{cmax}= 80 µmol m^{-2} s^{-1}, J=132 µmol m^{-2} s^{-1} and R_d =1 µmol m^{-2} s^{-1}.
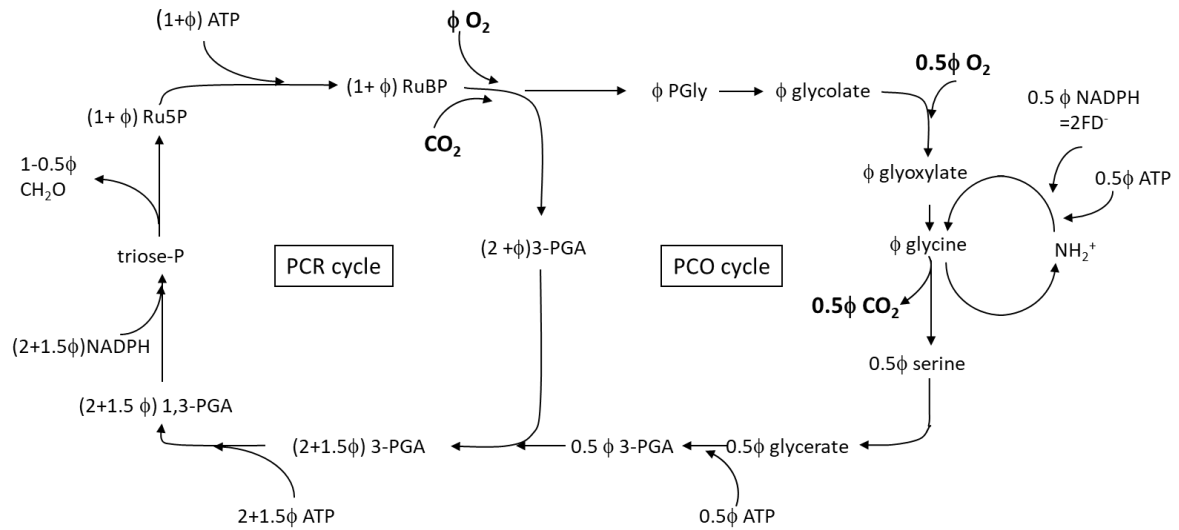
Figure 2

The stoichiometry of the photosynthetic carbon reduction (PCR) cycle and the photorespiratory carbon oxidation (PCO) cycle. Note that the regeneration of 0.5 mol of PGA from 1 mol PGly requires the 0.5 mol ATP. It also includes the release and refixation 0.5 mol of ammonia which requires 1 mol of reduced ferredoxin which in terms of electron transport is equivalent to 0.5 mol of NADPH and 0.5 mol of ATP (Keys et al., 1978) The stoichiometry and diagram are adapted from Farquhar et al. (1980).
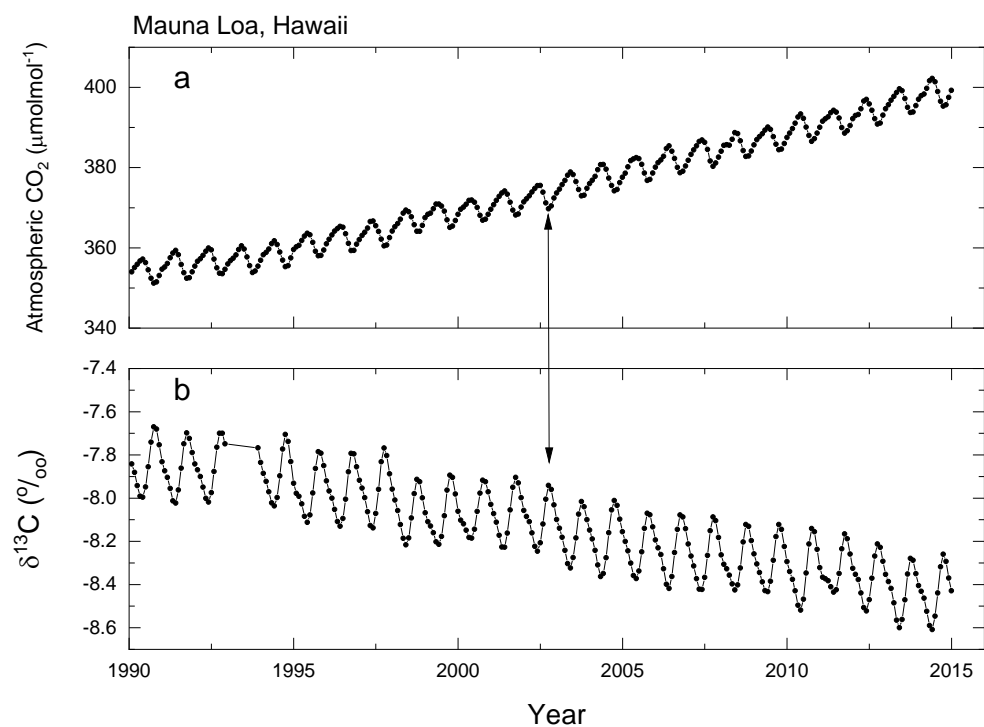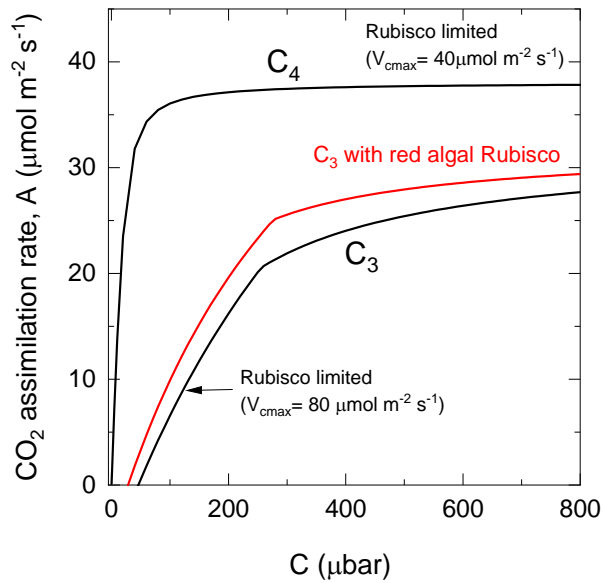
Figure 3

Monthly averages of atmospheric CO_2 (a) and the carbon isotope composition of atmospheric CO_2 (b) sampled in flasks at Mauna Loa, Hawaii. Data were downloaded from www.cmdl.noaa.gov (Dlugokencky et al., 2019; White et al., 2018). The figure illustrates the rising atmospheric CO_2 concentration together with the inter-annual oscillation. Increased photosynthesis in the summer months results in a decrease in atmospheric CO_2. Rubisco's action is apparent in (b) from the increase in $\delta^{13}C$ which indicates an increase $^{13}CO_2$ in the atmosphere as Rubisco preferentially fixes $^{12}CO_2$. ($\delta^{13}C$ is defined as $\frac{^{13}C}{^{12}C} air \bigg/ \frac{^{13}C}{^{12}C} std - 1$, where the standard it PBD belemnite (Farquhar et al., 1989)).

Figure 4
Click here to download Figure: Figure 4.docx

Figure 4

Modelled response of CO_2 assimilation rate, A versus chloroplast (C_3) or mesophyll (C_4) CO_2 partial pressure, C at 200 mbar O_2. For C_3 photosynthesis the model uses equations 9 and 11 with K_C=260 µbar K_O=179 mbar and Γ*= 38.6 µbar. V_{cmax}= 80 µmol m^{-2} s^{-1} and J=132 µmol m^{-2} s^{-1} and R_d =1 µmol m^{-2} s^{-1}. The Rubisco kinetic constants for the red algal Rubisco (*Griffithsia monilis*) were taken from Fig. 4 (Sharwood, 2017). Expressed in the gaseous phase K_C=278 µbar K_O=563 mbar and Γ*= 22.6 µbar. V_{cmax}= 67 µmol m^{-2} s^{-1} and J=132 µmol m^{-2} s^{-1} and R_d =1 µmol m^{-2} s^{-1}. The V_{cmax} is lower to keep the same Rubisco site content for both C_3 curves of 25.8 µmol m^{-2}. The A-C curve for C_4 photosynthesis uses the model equations from von Caemmerer (2000) together with the PEP carboxylase and Rubisco kinetic constants from *Setaria viridis* (Boyd et al., 2015). K_C=1210 µbar K_O=292 mbar and Γ*= 76.3 µbar. V_{cmax}= 40 µmol m^{-2} s^{-1} and the PEP carboxylase parameters are V_{pmax}= 300 µmol m^{-2} s^{-1}, The K_m CO_2 for PEPC, K_p=154 µbar and a bundle sheath conductance to CO_2 of 3 mmol m^{-2} s^{-1} bar^{-1} (Alonso-Cantabrana et al., 2018). Note that a V_{cmax}= 40 µmol m^{-2} s^{-1} corresponds to a Rubisco site content of 7.35 µmol m^{-2}.